

Quantum Chemical Studies of Model Cytochrome P450 Oxidations of Amines. 1. MNDO Pathways for Alkylamine Reactions with Singlet and Triplet Oxygen

Amiram Goldblum[†] and Gilda H. Loew*

Contribution from the Department of Pharmaceutical Chemistry, The Hebrew University School of Pharmacy, Jerusalem 91120, Israel, and the Life Sciences Division, SRI International, Menlo Park, California 94025. Received July 17, 1984

Abstract: Reaction pathways for oxidation of ammonia and mono-, di-, and trimethylamine by singlet and triplet oxygen atoms as models for cytochrome P450 enzymatic oxidation have been characterized by using the semiempirical molecular orbital method MNDO. Enthalpies and entropies of formation have been calculated for reactants, transition states, intermediates, and products on closed-shell and triplet pathways, and free energies of reaction and activation have been calculated from them. Energy minima and transition states have been verified by calculation of force constants. The results indicate a two-step, addition-rearrangement mechanism for nonradical oxidation leading to both *N*-hydroxy and *N*-methoxy products via *N*-oxide intermediates. While barriers to the rearrangement are higher than to *N*-oxide formation, the first step is determining the overall reaction in the gas phase. On a triplet surface, both α -C- and *N*-oxidation are competitive. *N*-Oxidation via an addition mechanism appears to be favored over an H-abstraction mechanism. However, in contrast to a closed-shell mechanism, no stable *N*-oxide radical intermediate is found, and the barrier to formation of *N*-hydroxy and *N*-methoxyl products on a triplet surface is greater. Additional gas phase, solution, and enzymatic studies, particularly focusing on identification of transient intermediates and products, are necessary to further distinguish among these mechanisms.

A large number of synthetic drugs and environmental chemicals contain free or substituted amino groups. Many of those are arylamines, producing toxic effects which have been attributed to their metabolic transformation products following enzyme oxidations.¹ *N*-Hydroxylamines² and *N*-oxides³ were suspected of inducing cancer, and much research has been devoted to the identification of those and other metabolites. The two major metabolic pathways involving amino groups are *N*-oxidation and oxidative dealkylation. *N*-Oxidation was found for primary,⁴ secondary, and tertiary³ amines in mammalian liver microsomes and was proposed to be more important in human liver⁵ than in laboratory animals. A flavin-dependent *N*-oxidase⁶ devoid of iron, copper, and cytochromes was isolated from pig liver microsomes and shown to catalyze *N*-oxidation of secondary and tertiary alkyl- and arylamines.⁷ Primary alkylamines were not oxidized, but they did give *N*-oxidized metabolites in other microsomal preparations.⁸

In view of these findings, it is yet unclear to what extent P450 participates in *N*-oxidations of amines. Two separate enzymatic routes have been suggested for alkylamine oxidations.⁸ One is *N*-dealkylation following an α -C oxidation (*N*-alkylol formation) and another is *N*-oxidation forming *N*-oxides and hydroxylamines. While *N*-oxides have been isolated in liver microsomes^{8,9} only for tertiary amine substrates, they are assumed to precede hydroxylamine formation in other amines. Very few data are available for rates of biological *N*-oxidations, but *N*-alkylanilines were found to undergo oxidation faster than aniline.¹⁰

The nature of the oxygen atom transferred enzymatically to organic substrates is unknown. While oxygenase reactions resemble those of singlet carbene and nitrene, the production of free singlet oxygen atoms from O₂ is highly improbable, being largely endothermic. The much less endothermic reaction to form a triplet ground-state oxygen atom is, in principle, feasible in the presence of appropriate biological reducing agents.¹¹ The spin state of an enzymatically bound oxygen atom may vary with the enzymatic system involved.

In gas-phase studies of amine reactions with oxygen atoms,¹² O-amine adducts were detected for methylamine and dimethylamine as the species preceding further fragmentation. Hydrogen abstraction from nitrogen was found only for (C-D₃)₂NH, and indications were found that the abstraction process

follows addition in dimethyl- and trimethylamine.

The various pathways available for oxygen atom reactions with amines were compared in a previous theoretical semiempirical study of O(¹S) with methylamine.¹³ The enthalpy for *N*-oxide formation is largely favored, in vacuo, with respect to H abstraction and insertion to N-H bonds. A much lower barrier to hydrogen abstraction was predicted for H₃O⁺ assisted reactions. A singlet bound state for ammonia oxide was found by ab initio studies, which predicted a highly repulsive surface for NH₃ + O(³P).¹⁴ Accurate ab initio studies for oxygen reactions with amines may be feasible, but even these small system calculations become costly¹⁵ when total optimizations of all structures must be considered.

Following recent achievements in applying semiempirical MNDO-SCF-MO¹⁶ calculations to complex reactions,¹⁷⁻¹⁹ we

- (1) Bridges, J. W.; Gorrod, J. W.; Parke, D. V., Eds. "Biological Oxidation of Nitrogen in Organic Molecules"; Taylor and Francis: London, 1972.
- (2) Bartsch, H.; Dworkin, M.; Miller, J. A.; Miller, E. C. *Biochem. Biophys. Acta* **1972**, *286*, 272.
- (3) Bickel, M. H. *Pharmac. Rev.* **1969**, *21*, 325.
- (4) Miller, J. A.; Miller, E. C. *Prog. Exp. Tumor Res.* **1969**, *11*, 273.
- (5) Ziegler, D. M.; Gold, M. S., ref 1, p 13.
- (6) Ziegler, D. M.; Mitchell, C. H.; Jollow, D. In "Microsomes and Drug Oxidation"; Gillette, J. R., Conney, A. H., Cosmides, G. J., Estabrook, R. V., Fouts, J. R., Mannering, G. J., Eds.; Academic Press: New York, 1969; p 173.
- (7) Ziegler, D. M.; Poulsen, L. L.; Mckee, E. M., ref 1, p 211.
- (8) Beckett, A. H., ref 1, p 53.
- (9) Baker, J. R.; Chaykin, S. *J. Biol. Chem.* **1960**, *237*, 1309.
- (10) Uehleke, H. In "Proceedings of the First International Pharmacological Meeting"; Brodie, B. B., Erdős, E. G., Eds.; Pergamon Press: Oxford, 1961; Vol. 6; p 31.
- (11) Hamilton, G. A. In "Molecular Mechanisms of Oxygen Activation"; Hayaishi, O. Ed.; Academic Press: New York, 1974.
- (12) Slagle, I. R.; Dudich, J. F.; Gutman, D. *J. Phys. Chem.* **1979**, *83*, 3065.
- (13) Pack, G. R.; Loew, G. H. *Int. J. Quantum Chem., Quantum Biol. Symp.* **1979**, *6*, 381.
- (14) Hart, B. T. *Aust. J. Chem.* **1976**, *29*, 231.
- (15) Walch, S. P.; Dunning, T. H., Jr. *J. Chem. Phys.* **1980**, *72*, 3221.
- (16) Dewar, M. J. S.; Thiel, W. *J. Am. Chem. Soc.* **1977**, *99*, 4899.
- (17) Brown, S. B.; Dewar, M. J. S.; Ford, G. P.; Nelson, D. J.; Rzepa, H. S. *J. Am. Chem. Soc.* **1978**, *100*, 7832.
- (18) Oie, T.; Loew, G. H.; Burt, S. K.; Binkley, J. S.; MacElroy, R. D. *J. Am. Chem. Soc.* **1982**, *104*, 6169.

[†] The Hebrew University School of Pharmacy.

* Address correspondence to this author at SRI International.

report here a theoretical study of the kinetics and thermodynamic pathways of model amine oxidations by singlet and triplet oxygen. While keeping in mind the limitations of such a "gas-phase" approach to the resolution of complex biological reactions and the unavailability of appropriate reference experimental studies, theoretical model studies may nevertheless be helpful for the qualitative interpretation of enzyme reactions and to suggest further experimental studies.

Theoretical Methods

As the theoretical framework for semiempirical calculations of kinetic and thermodynamic quantities on reaction pathways were previously described in detail,¹⁹ only a brief account follows:

(1) Reactants and products are connected by a reaction path, first characterized at intervals along appropriately chosen "reaction coordinates", while all other internal (R, θ, ϕ) coordinates undergo total optimization. The totally optimized reactants and products are then identified as stationary points having only positive eigenvalues of the force constant matrix. Transition states are identified as the lowest "saddle point" connecting reactants and products and having a single negative eigenvalue of the force constant (FC) matrix. MNDO is parameterized to obtain heats of formation, and thus the enthalpies for all the molecular species involved may be obtained.

(2) Calculated positive vibrational frequencies are used for constructing the vibrational partition function, while the TS mode negative eigenvalue vector identifies the nuclear displacements of the "reaction coordinate" for conversion between reactants and products.

(3) Rotational principal moments of inertia are calculated at the optimized geometries of all species for the evaluation of rotational partition functions.

(4) Entropies of formation were calculated by standard formulae of statistical mechanics,²⁰ including symmetry corrections for external and internal ("rotor") rotations.²¹ However, nitrogen inversion and optical isomers were not accounted for.

(5) Reaction free energies (ΔG_r) were calculated by

$$\Delta H_r = \sum_i^{\text{products}} \Delta H_f(i) - \sum_j^{\text{reactants}} \Delta H_f(j) \quad (a)$$

$$\Delta S_r = \sum_i^{\text{products}} S(i) - \sum_j^{\text{reactants}} S(j) \quad (b)$$

$$\Delta G_r = \Delta H_r - T\Delta S_r \quad (c)$$

Similarly, activation free energies (ΔG^\ddagger) were calculated by difference in enthalpies and entropies between transition states and reactants.

Absolute and relative rates have been determined by the Eyring equation²¹ for the following rate constants—(1) $k = 1.5199 \times 10^{17} \times \exp(-\Delta G^\ddagger/0.5925)$ cm³/(mol·s), with ΔG^\ddagger expressed in kcal/mol.

A UHF-based formalism²² was used for all calculations involving open-shell species. In the triplet reactions small (<0.01) "spin contaminations" ($S^2 > 2.000$) were found, thus minimizing a well-known defect of this formalism.

As no clearly defined experimental enthalpies and entropies for amine oxidations are available, it is not possible to assess the reliability of the MNDO results for the studied reactions. Previous studies of O(³P) oxidations of CH₄ and C₂H₄²³ found it to overestimate activation enthalpies to different extents, while activation entropies were in close agreement with experiments. It is hoped that if such overestimations exist in the present set of calculations, they will be partly eliminated in comparisons of activation energies for different molecules undergoing similar reactions.

All the studies reported here use the semiempirical molecular orbital method MNDO, NDTs, NDFOR^{16,24,26} for geometry optimizations, tran-

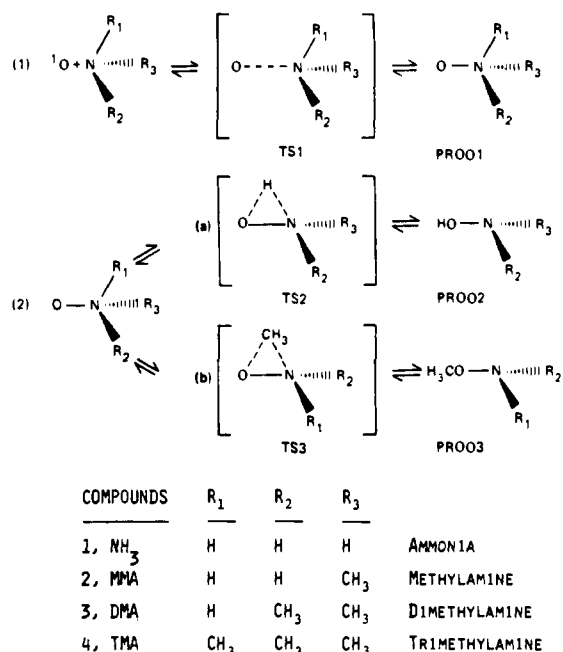


Figure 1. Pathway for N-oxidation of alkylamines by singlet oxygen: (1) N-oxide formation, (2) rearrangement of N-oxide to form (a) hydroxylamine and (b) methoxyamine.

Table I. Reaction Thermodynamics for N-Oxide Formation at 298 K

| reaction | ΔH_r , kcal/mol | ΔS_r , cal/(mol·deg) | ΔG_r , kcal/mol |
|---|-------------------------|------------------------------|-------------------------|
| (1) ¹ O + NH ₃ → ONH ₃ | -85.92 | -30.77 | -76.74 |
| (2) ¹ O + NH ₂ CH ₃ → ONH ₂ CH ₃ | -81.10 | -32.36 | -71.45 |
| (3) ¹ O + NH(CH ₃) ₂ → ONH(CH ₃) ₂ | -75.20 | -33.85 | -65.11 |
| (4) ¹ O + N(CH ₃) ₃ → ON(CH ₃) ₃ | -68.19 | -37.95 | -56.88 |

sition states, force constants, and THERMOG²⁵ for thermodynamic properties. This program has been carefully parameterized to give accurate enthalpies of formation at 298 K and geometries for a variety of organic molecules. A revised version of these programs has been developed in our laboratory which incorporates all these capabilities in one program.

Results

A. N-Oxidation of Aliphatic Amines by Singlet Oxygen. Figure 1 shows the addition–rearrangement reactions modeled for ammonia (NH₃), methylamine (MMA), dimethylamine (DMA), and trimethylamine (TMA) with singlet oxygen forming hydroxy (PROD2) or methoxy products (PROD3) via N-oxide intermediates (PROD1). A H rearrangement of N-oxide (pathway 2a) is not possible for TMA, while a methyl rearrangement—considered for the first time here—pathway 2b, is not possible for NH₃. Geometry-optimized reactants, transition states, and products were calculated for all the possible amine reactants for the three pathways 1, 2a, and 2b shown in Figure 1. Given in Figure 2 are typical optimized structures and net atomic charges for one reactant, methylamine, the transition state (TS1) found for its N-oxide formation, and its N-oxide product (PROD1). The arrows indicate the relative nuclear displacement in the TS vibrational mode corresponding to the reaction coordinate. (Similar results for the other reactants are given in Figures 1S and 2S of the supplementary material.)

Reaction thermodynamics for N-oxide formation are given in Table I, while Table II gives the activation parameters, TS frequencies, and rates of these reactions. Quantities in these tables were obtained from the calculated thermochemical quantities given in the supplementary material (Table 1S) for all starting materials, for all transition states (IIaS), and for all products (IIbS) of pathway 1, singlet oxygen, and amine reactants forming N-oxide products. MNDO predictions for the enthalpies of formation for the parent amines differ from experimental values by ~3.0 kcal/mol while entropy values have an average error of ~2.5 eu.

(19) Flanigan, M. C.; Komornicki, A.; McIver, J. W., Jr. In "Modern Theoretical Chemistry"; Segal, G. A., Ed.; Plenum Press: New York, 1977; Vol. 8.

(20) Davidson, N. "Statistical Mechanics"; McGraw-Hill: New York, 1962.

(21) Benson, S. W. "Thermochemical Kinetics", 2nd ed.; Wiley-Interscience: New York, 1976.

(22) Pople, J. A.; Beveridge, D. L. "Approximate Molecular Orbital Theory"; McGraw-Hill: New York, 1970.

(23) Pudzianowski, A. T.; Loew, G. H. *Mol. Catal.* **1982**, *17*, 1.

(24) Thiel, W.; Ford, G. P.; McKee, M.; Nelson, D.; Olivella, S.; Rzepa, H.; Dewar, M. J. S.—programs were obtained from N.R.C.C. and modified in our laboratory by Dr. Dale Spangler.

(25) Ford, G. P.—obtained from N.R.C.C. and modified in our laboratory by Dr. Dale Spangler.

(26) Dewar, M. J. S.; Thiel, W. *J. Am. Chem. Soc.* **1977**, *99*, 4909.

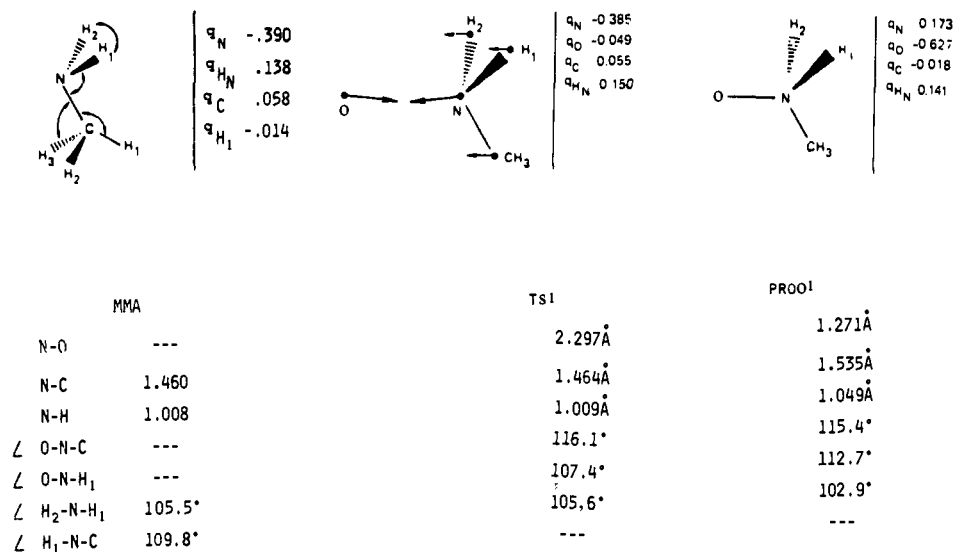


Figure 2. N-Oxidation of methylamine by singlet oxygen: Optimized MNDO geometries and their Mulliken net atomic charges (q_i) for parent compound, transition state (TS1), and product (PROD1) structure. The arrows on the transition states here and in the following figures indicate the direction and vector lengths for relative nuclear displacements in the vibrational mode corresponding to reaction coordinate.

Table II. Reaction Kinetics for N-Oxide Formation at 298 K

| reaction no. | ΔH^\ddagger , kcal/mol | ΔS^\ddagger , cal/(mol-deg) | ΔG^\ddagger , kcal/mol | $-\omega^\ddagger$, cm ⁻¹ | rate constant, cm ³ /(mol-s) | rel rate |
|--------------|--------------------------------|-------------------------------------|--------------------------------|---------------------------------------|---|----------|
| (1) | 2.44 | -27.42 | 10.62 | 253 | 2.51×10^9 | 1900 |
| (2) | 2.94 | -27.52 | 11.14 | 281 | 1.03×10^9 | 800 |
| (3) | 4.00 | -29.12 | 12.68 | 287 | 7.67×10^7 | 60 |
| (4) | 5.60 | -31.83 | 15.09 | 315 | 1.32×10^6 | 1 |

Table III. Reaction Thermodynamics for N-Oxide Rearrangement to Hydroxylamines at 298 K

| reaction | ΔH_r , kcal/mol | ΔS_r , cal/(mol-deg) | ΔG_r , kcal/mol |
|--|-------------------------|------------------------------|-------------------------|
| (5) ONH ₃ → HO-NH ₂ | -42.70 | 3.13 | -43.63 |
| (6) ONH ₂ CH ₃ → HO-NHCH ₃ | -45.99 | 6.63 | -46.78 |
| (7) ONH(CH ₃) ₂ → HO-N(CH ₃) ₂ | -49.59 | 1.39 | -50.01 |

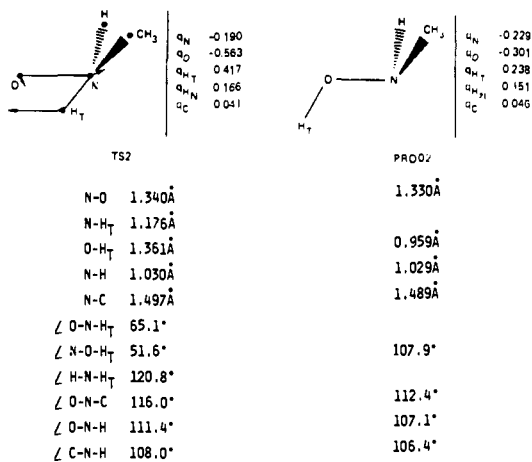


Figure 3. H rearrangement of N-oxides to hydroxylamines: Typical transition states (TS2) and products (PROD2) for hydrogen transfer from N to O in monomethyl N-oxide to form hydroxylamines.

Subsequent rearrangement of the N-oxides (PROD1) to hydroxylamines (PROD2, pathway 2a) was considered for NH₃,

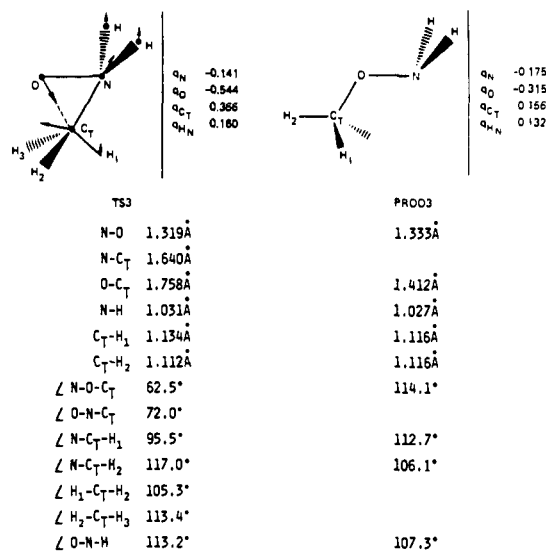


Figure 4. Typical transition state (TS3) and product (PROD3) for methyl transfer from N to O in monomethyl N-oxides to form N-methoxyamines.

MMA, and DMA. Figure 3 shows the corresponding TS (TS2) and product (PROD2) structures and charges for the methylamine reactant. All other structures are available in the supplementary material (Figure 3S). Thermochemical quantities for TS2 and PROD2 in pathway 2a are presented in Table IIIS, while reaction thermodynamics and activation parameters are given in Tables III and IV, respectively.

Table IV. Activation Parameters and Rates for N-Oxide Rearrangement to Hydroxylamines at 298 K

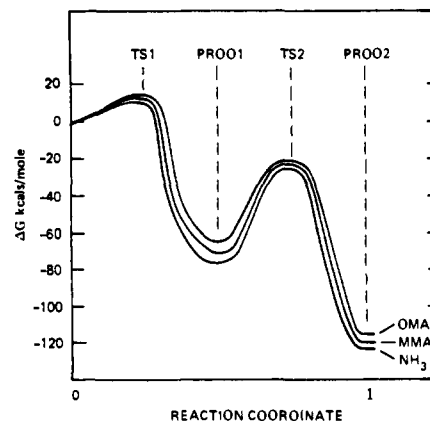
| reaction no. | ΔH^\ddagger , kcal/mol | ΔS^\ddagger , cal/(mol-deg) | ΔG^\ddagger , kcal/mol | $-\omega^\ddagger$, cm ⁻¹ | rate constant, cm ³ /(mol-s) | rel rate |
|--------------|--------------------------------|-------------------------------------|--------------------------------|---------------------------------------|---|----------|
| (5) | 49.75 | 2.35 | 49.05 | 2452 | 1.68×10^{-19} | 1 |
| (6) | 46.50 | 1.98 | 45.91 | 2435 | 3.35×10^{-17} | 200 |
| (7) | 43.59 | 0.84 | 43.34 | 2428 | 2.57×10^{-15} | 1500 |

Table V. Reaction Thermodynamics for *N*-Oxide Rearrangement to *O*-Alkyl Hydroxylamines at 298 K

| reaction | ΔH_r^\ddagger , kcal/mol | ΔS_r^\ddagger , cal/ (mol-deg) | ΔG_r^\ddagger , kcal/mol |
|---|-------------------------------------|---|-------------------------------------|
| (8) $\text{ONH}_2\text{CH}_3 \rightarrow \text{CH}_3\text{ONH}_2$ | -41.90 | 2.17 | -42.54 |
| (9) $\text{ONH}(\text{CH}_3)_2 \rightarrow \text{CH}_3\text{ONHCH}_3$ | -48.10 | 3.25 | -49.07 |
| (10) $\text{ON}(\text{CH}_3)_3 \rightarrow \text{CH}_3\text{ON}(\text{CH}_3)_2$ | -54.63 | 5.40 | -56.24 |

The other available route for rearrangement of *N*-oxides is alkyl transfer (MMA, DMA, and TMA) from nitrogen to oxygen (pathway 2b). The results for this methyl-group transfer are given in Tables IVS, V, and VI, respectively, for thermochemical quantities, reaction thermodynamics, and kinetics. The corresponding transition-state and product (TS3, PROD3) structures are shown in Figure 4 for the methylamine reactant. All others are available in the supplementary material (Figure 4S).

B. *N*-Oxidation of Aliphatic Amines by $\text{O}(\text{^3P})$ Oxygen Addition Pathway. Triplet oxygen reactions with amine nitrogen corresponding to oxygen addition to the nitrogen were considered according to the general pathways depicted in Figure 6, following spin conservation rules. Table VS in the supplementary material contains MNDO calculated thermochemical quantities for the optimized TS structures (TS4), and for the radical intermediates (INT4) of all parent amines. Tables VII and VIII summarize

**Figure 5.** Energy profile for the conversion of amines to hydroxylamines (PROD2) by singlet oxygen oxidation via *N*-oxides (PROD1). The curves start at an identical reference energy ($\Delta G = 0.0$).

the thermodynamic and activation parameters calculated from these data for the addition reactions. Figure 7 shows the structure of TS4 and the radical intermediate (INT4a) along with Mulliken charge distribution and the distribution of unpaired spin density for methylamine. Results for all other parent amines are available

Table VI. Activation Parameters and Rates for *N*-Oxide Rearrangement to *O*-Alkyl Hydroxylamines, at 298 K

| reaction no. | ΔH^\ddagger , kcal/mol | ΔS^\ddagger , cal/ (mol-deg) | ΔG^\ddagger , kcal/mol | $-\omega^\ddagger$, cm^{-1} | rate constant $\text{cm}^3/(\text{mol}\cdot\text{s})$ | rel rate |
|--------------|-----------------------------------|---|-----------------------------------|---------------------------------------|--|-----------------|
| (8) | 48.07 | 1.54 | 47.61 | 989 | 1.9×10^{-18} | 1 |
| (9) | 42.94 | 2.24 | 42.27 | 942 | 1.6×10^{-14} | 8×10^3 |
| (10) | 38.19 | 6.70 | 36.19 | 914 | 4.0×10^{-10} | 2×10^8 |

Table VII. Reaction Thermodynamics for $\text{O}(\text{^3P})$ Addition Reactions with Amines, at 298 K

| reaction | $\Delta H_{\text{rad}}^\ddagger$, kcal/mol | $\Delta S_{\text{rad}}^\ddagger$, cal/ (mol-deg) | $\Delta G_{\text{rad}}^\ddagger$, kcal/mol | $\Delta H_{\text{recomb}}^\ddagger$, kcal/mol | $\Delta G_{\text{overall}}^\ddagger$, kcal/mol |
|--|--|--|--|---|--|
| (11) $\text{O}(\text{^3P}) + \text{NH}_3 \rightarrow \text{ONH}_2^\cdot + \text{H}\cdot \rightarrow \text{HONH}_2$ | 3.48 | -0.37 | 3.58 | -78.82 | -66.77 |
| (12) $\text{O}(\text{^3P}) + \text{NH}_2\text{CH}_3 \rightarrow \text{ONHCH}_3^\cdot + \text{H}\cdot \rightarrow \text{HONHCH}_3$ | 2.90 | -2.89 | 3.76 | -76.72 | -64.63 |
| (12a) $\text{O}(\text{^3P}) + \text{NH}_2\text{CH}_3 \rightarrow \text{ONH}_2^\cdot + \text{CH}_3^\cdot \rightarrow \text{CH}_3\text{ONH}_2$ | -22.79 | 9.16 | -25.52 | -46.93 | -59.74 |
| (13) $\text{O}(\text{^3P}) + \text{NH}(\text{CH}_3)_2 \rightarrow \text{ON}(\text{CH}_3)_2^\cdot + \text{H}\cdot \rightarrow \text{HON}(\text{CH}_3)_2$ | 2.53 | -1.97 | 3.12 | -74.05 | -61.51 |
| (13a) $\text{O}(\text{^3P}) + \text{NH}(\text{CH}_3)_2 \rightarrow \text{ONCH}_3^\cdot + \text{CH}_3^\cdot \rightarrow \text{CH}_3\text{ONHCH}_3$ | -25.45 | 12.50 | -29.17 | -44.58 | -59.27 |
| (14) $\text{O}(\text{^3P}) + \text{N}(\text{CH}_3)_3 \rightarrow \text{ON}(\text{CH}_3)_2^\cdot + \text{CH}_3^\cdot \rightarrow \text{CH}_3\text{ON}(\text{CH}_3)_2$ | -28.77 | 15.81 | -33.48 | -40.78 | -59.52 |

Table VIII. Activation Parameters and Rates for $\text{O}(\text{^3P})$ Addition Reactions with Amines at 298 K

| reaction no. | ΔH^\ddagger , kcal/mol | ΔS^\ddagger , cal/ (mol-deg) | ΔG^\ddagger , kcal/mol | $-\omega^\ddagger$, cm^{-1} | rate constant, $\text{cm}^3/(\text{mol}\cdot\text{s})$ |
|--------------|-----------------------------------|---|-----------------------------------|---------------------------------------|--|
| (11) | 24.33 | -31.15 | 33.61 | 1189 | 3.51×10^{-8} |
| (12) | 24.53 | -28.38 | 32.99 | 465 | 9.90×10^{-8} (0.6×10^{-12}) ^a |
| (13) | 28.95 | -31.26 | 38.27 | 609 | 1.33×10^{-11} (6.1×10^{-12}) ^a |
| (14) | 35.57 | -34.00 | 45.71 | 784 | 4.37×10^{-17} (22×10^{-12}) ^a |

^a From ref 37, see text.

Table IX. Reaction Thermodynamics for Hydrogen Abstractions from Methylamine by $\text{O}(\text{^3P})$ at 298 K and Comparisons to *N*-Oxidation

| reaction | $\Delta H_{\text{rad}}^\ddagger$, kcal/mol | $\Delta S_{\text{rad}}^\ddagger$, cal/ (mol-deg) | $\Delta G_{\text{rad}}^\ddagger$, kcal/mol | $\Delta H_{\text{recomb}}^\ddagger$, kcal/mol | $\Delta G_{\text{overall}}^\ddagger$, kcal/mol |
|--|--|--|--|---|--|
| (15) $\text{O}(\text{^3P}) + \text{NH}_2\text{CH}_3 \rightarrow \text{NH}_2\text{CH}_2^\cdot + \text{OH}\cdot \rightarrow \text{NH}_2\text{CH}_2\text{OH}$ | -34.48 | 9.09 | -37.19 | -72.92 | -98.40 |
| (16) $\text{O}(\text{^3P}) + \text{NH}_2\text{CH}_3 \rightarrow \text{NHCH}_3^\cdot + \text{OH}\cdot \rightarrow \text{HONHCH}_3$ | -22.38 | 9.75 | -25.29 | -51.44 | -73.82 |
| (12) ^a $\text{O}(\text{^3P}) + \text{NH}_2\text{CH}_3 \rightarrow \text{ONHCH}_3^\cdot + \text{H}\cdot \rightarrow \text{HONHCH}_3$ | 2.90 | -2.89 | 3.76 | -76.72 | -64.63 |
| (12a) ^a $\text{O}(\text{^3P}) + \text{NH}_2\text{CH}_3 \rightarrow \text{ONH}_2^\cdot + \text{CH}_3^\cdot \rightarrow \text{CH}_3\text{ONH}_2$ | -22.79 | 9.16 | -25.52 | -46.93 | -59.74 |

^a Reactions given in Table VII and presented again for comparison.

Table X. Activation Parameters and Rates for $\text{O}(\text{^3P})$ Hydrogen Abstractions from Methylamine at 298 K

| reaction no. | ΔH^\ddagger , kcal/mol | ΔS^\ddagger , cal/(mol-deg) | ΔG^\ddagger , kcal/mol | $-\omega^\ddagger$, cm^{-1} | rate constant, $\text{cm}^3/(\text{mol}\cdot\text{s})$ | rel rate |
|-------------------|-----------------------------------|--|-----------------------------------|---------------------------------------|---|-------------------|
| (15) | 25.83 | -21.94 | 32.37 | 2417 | 2.84×10^{-7} | 3.6×10^6 |
| (16) | 33.65 | -25.73 | 41.32 | 3494 | 7.79×10^{-14} | 1 |
| (12) ^a | 24.53 | -28.38 | 32.99 | 465 | 9.90×10^{-8} | 1.3×10^6 |

^a From Table VIII, presented here for comparison.

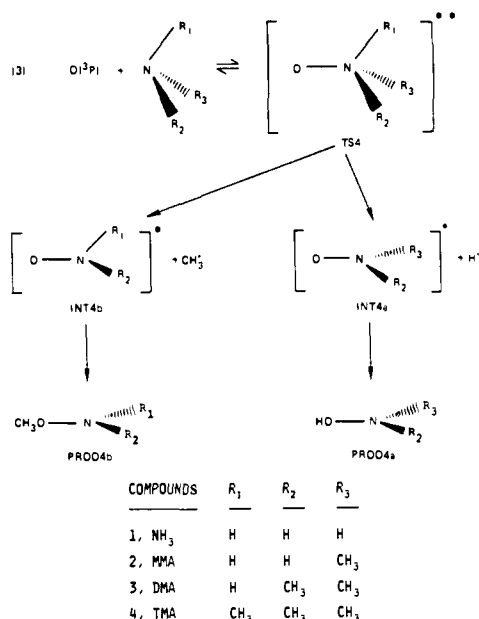


Figure 6. Pathways for N-oxidation of alkylamines by O(³P).

in the supplementary material (Figure 5S).

C. O(³P) Hydrogen Abstraction from N-H and C-H in Methylamine. As indicated in Figure 9, as well as modeling the addition of oxygen to nitrogen, hydrogen abstractions by triplet oxygen (a) from the α -C and (b) from the nitrogen atoms of methylamine were modeled leading to *N*-alkylol (PROD5) and *N*-methylhydroxylamine (PROD6) products. Thermochemical quantities, reaction thermodynamics, and activation parameters for these reactions are given in Tables VIS, IX, and X, while Figure 10 shows the TS (TS5 and TS6) and products (5 and 6) obtained, including their geometry, spins, and charges.

Discussion

Closed-shell reactions of oxygen atom with a series of methylamines have been characterized. The results indicate that such nonradical oxidation occurs by a two-step addition-rearrangement mechanism leading to both *N*-hydroxylamine and *N*-methoxyamine products via *N*-oxide intermediates. Neither H abstraction nor insertion pathways were found on the closed-shell singlet surface.

The interaction of aliphatic amines with singlet oxygen to form *N*-oxides is calculated to be very exothermic (Table I) and to have relatively low activation barriers (Table II). The transition states have long (>2.2 Å) N-O "bonds" resembling the reactants (Figure 2) which become, however, progressively shorter than additional alkyl substitution. A characteristic low frequency ($\omega^* \approx -275$) accompanies the TS modes. The exothermicity of the reaction decreases with increasing alkyl substitution due to an increase in the enthalpy of formation of the *N*-oxides. The relative rates follow the trend in ΔG_r —faster reactions are predicted for increasingly exothermic ones. The *N*-oxides formed have 55 to 75 kcal/mol excess energy and, in the gas phase, under collision-free conditions, would constitute highly excited energy rich intermediates.

It should be noted that singlet oxygen, which is a mixture of ¹D and ¹S states,²⁷ is represented in the calculations by a single configuration description closer in enthalpy to the O(¹D) value. O(¹S) is 51.2 kcal/mol higher in enthalpy. Using this value in the calculations raises the exothermicity of the first step, *N*-oxide formation, considerably and leads to no energy barrier.

As seen in Figure 2, some charge is transferred to oxygen in the TS, most effectively by hydrogens attached to N. This negative charge on the oxygen increases substantially in the *N*-oxide

products so that the nitrogen becomes positive. This result verifies the validity of the O⁻N⁺ notation commonly used for *N*-oxides. However, MNDO probably overestimates the charge polarity, as it also underestimates the bond length, 1.278 vs. 1.388 Å found for N-O in TMA.²⁹ Ab initio calculations with gaussian lobe functions found for NH₃ + O(¹D)¹⁴ a stable *N*-oxide with a long N-O bond (1.69 Å, compared to an STO-3G³⁰ value of 1.582 Å, and a MNDO value of 1.268 Å) and no barrier to the reaction ($\Delta E = -34.0$ kcal/mol). Hydrogen charge transfer was large ($q_H = 0.255$ in NH₃ and 0.319 in O-NH₃¹⁴). Such differences in charge distribution may partly account for the erroneous predictions by MNDO of hydrogen bonding distances and interaction,^{13,31} having long H bonds and wrong geometries.

As shown in Tables III and IV, the rearrangement of *N*-oxides to hydroxylamines is exothermic but requires large activation energies. The transition states shown in Figure 3 indicate that the hydrogen transfer is unsymmetrical, being closer to N than to O, despite the large charges on both O and H. The different amines have very similar transition states as expressed in bond lengths and angles, as well as reaction coordinate frequencies (ω^*) and charges. Most of the free energy of activation and of reaction stems from the enthalpies, while activation and reaction entropies are small.

As shown in Figure 5, though the theoretically calculated gas-phase rates are infinitely small for these rearrangements (step 2), enough internal energy is gained in the initial oxidation step to overcome the activation barrier in the second step, despite the finding that rearrangement (TS2) is the "rate-determining step" on the singlet oxygen reaction surface with amines to form hydroxylamines. The initial small difference in ΔG^* which favors *N*-oxide formation in the sequence NH₃ > MMA > DMA is thus determining, although the order is reversed for the second transition state.

The other available route of rearrangement of *N*-oxides is alkyl transfer (MMA, DMA, and TMA) from nitrogen to oxygen. Such a rearrangement has been observed experimentally for benzyl dimethyl *N*-oxides,³² with benzyl migration. In another instance,³³ alkyl groups migrated when no β -hydrogens were present so that a "Cope rearrangement"³⁴ could not take place. As shown in Table V, the reactions become more exothermic with additional alkyl groups in a manner parallel to the hydrogen rearrangements (Table III). This same trend is seen also for the kinetics (Table X), with a smaller activation barrier for increased alkyl substitution. While both H transfer and CH₃ transfer are competitive, *N*-hydroxylamine formation is favored for monomethylamine (MMA), while *N*-methoxyamine formation is favored for dimethylamine (DMA).

Transition-state charges and dipole moments are larger for hydrogen than for methyl migration ($\mu = 3.62$ D, vs. 2.99 D for MMA; 3.67 D vs. 3.11 D for DMA), so that hydroxylamine formation may be favored in more polar environments. Generally, a reduction in polarity accompanies both reactions from the polar ($\mu > 5.0$ D) *N*-oxides to the nonpolar ($\mu = 0.2$ to 0.7 D) hydroxylamines and *O*-alkylhydroxylamines. In an analogous rearrangement of nitrones to oxime *O*-ethers, this reduction in polarity was suggested to be responsible for an unusual positive ($\Delta S^* + 13.6$) entropy of activation by causing an increase in the randomness of water molecules which are less attached to the TS.³⁴ A smaller, but positive, entropy is also calculated for the rearrangements studied here, with no solvent present. An exothermic reaction energy of -40 kcal/mol was found for the nitron rearrangement, quite similar to those calculated for both hydrogen and methyl rearrangements.

Two pathways for alkylamine N-oxidation by radical (³P) oxygen species have been characterized: an N-addition and an

(27) Moore, C. E. "Atomic Energy Levels"; National Bureau of Standards: Washington, D. C., 1945.

(28) Stull, D. R.; Westrum, E. F., Jr.; Sinke, G. C. "The Chemical Thermodynamics of Organic Compounds"; Wiley: New York, 1969.

(29) Caron, A.; Patenik, G. J.; Goldish, E.; Donhue, J. *Acta Crystallogr.* **1964**, *17*, 102.

(30) Lathan, W. A.; Curtiss, L. A.; Hehre, W. J.; Lisle, J. B.; Pople, J. A. *Prog. Phys. Org. Chem.* **1974**, *11*, 175.

(31) Scheiner, S. *Theor. Chem. Acta (Berlin)* **1980**, *57*, 71.

(32) Meisenheimer, J. *Chem. Ber.* **1919**, *52*, 1617.

(33) Bruaman, J. I.; Sanderson, W. A. *Tetrahedron* **1967**, *23*, 37.

(34) Cope, A. C.; Haven, A. C., Jr. *J. Am. Chem. Soc.* **1950**, *72*, 4896.

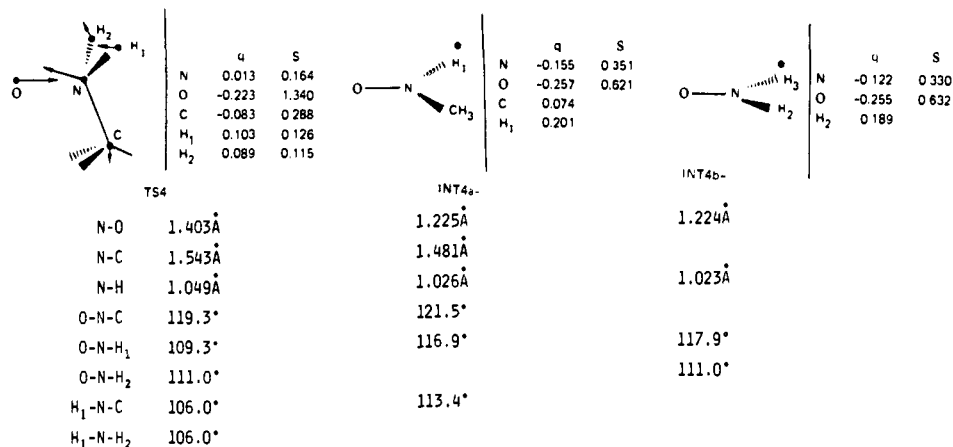


Figure 7. N Oxidation of amines by O(³P): Typical transition state (TS4) and intermediate (INT4a,4b) structures, charges (q_i), and spin densities (S) for methylamine.

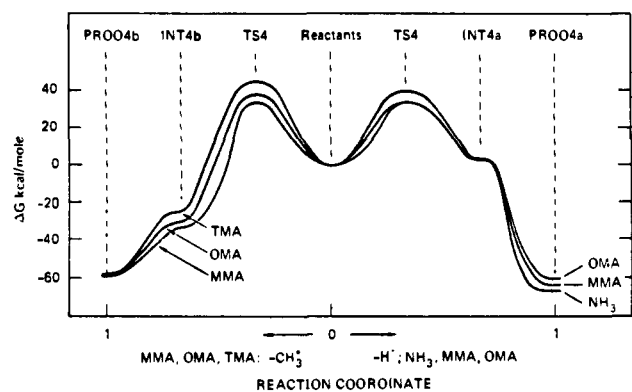


Figure 8. Energy profile for O(³P) N-oxidations of amines, from reactants at a reference energy value (center) to oxygen addition and hydrogen atom dissociation leading to hydroxylamines (right side) or methyl radical dissociation leading to methoxyamines (left).

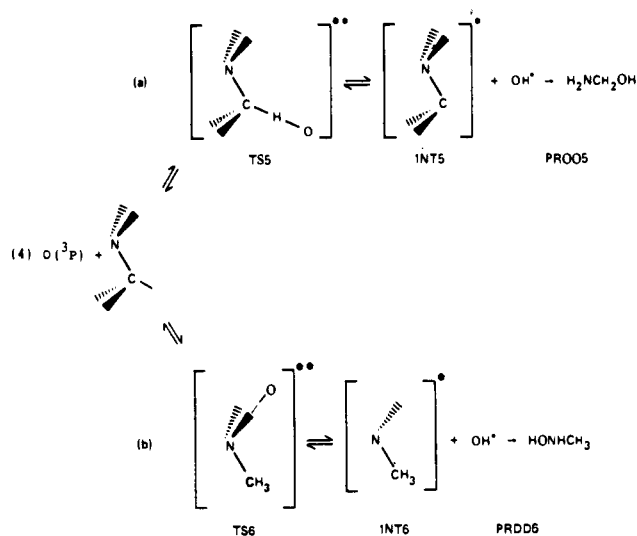


Figure 9. Pathways for H abstractions from C and N atoms of methylamine by O(³P).

N-H abstraction pathway and, for comparison, an α -C oxidation by H abstraction. As shown in Figure 7, in contrast to the closed-shell pathway, oxygen addition to nitrogen via a radical pathway leads to a tightly coupled transition state (TS4) with much shorter $r(\text{N-O})$ distances (1.30 to 1.47 Å) and a larger reaction coordinate vibrational frequency. Moreover, this transition state does not lead to formation of a stable triplet *N*-oxide intermediate. Instead, as indicated in Figure 6, intermediates are formed by addition of oxygen to the nitrogen and simultaneous

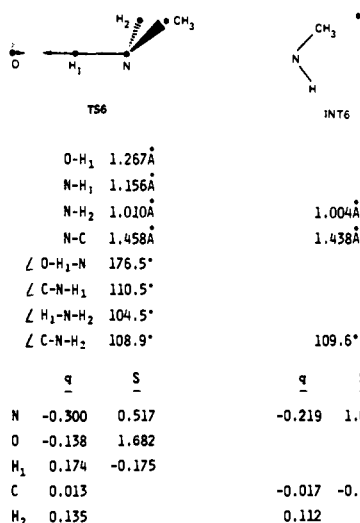
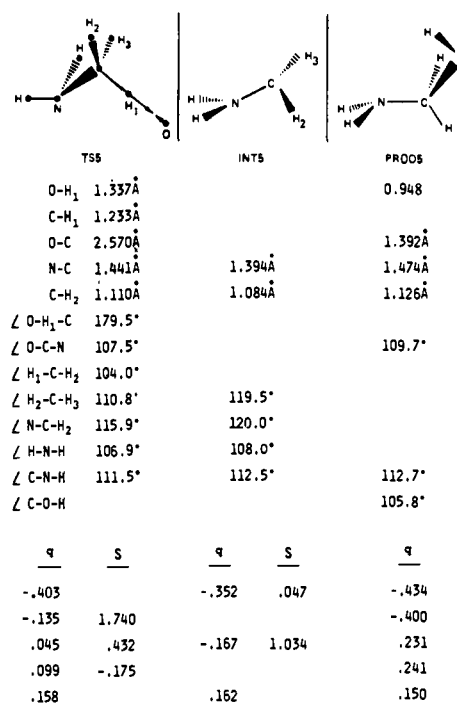


Figure 10. Transition states, intermediates, and products for H abstractions from (a, top) α -carbon and (b, bottom) nitrogen atoms of methylamine.

loss of either a hydrogen (INT4a) or methyl radical (INT4b). Radical recombination, presumably rapid compared to oxygen addition, then leads to hydroxy- or methoxyamine products (PROD4a,4b).

The assumption of a similar transition state (TS4 in Figure 6S) for the loss of H or CH₃ may be incorrect. This transition state may be compared for its ability to form both types of products only for MMA (TS4-2) and DMA (TS4-3 in Figure 7S). While the nuclear displacements of both CH₃ and H are in the direction of dissociation in TS4-2, TS4-3 is very different with respect to methyl vs. hydrogen displacements, with the methyl groups moving toward each other.

Large differences among the TS (TS4, Figure 7) are observed with respect to N–O bond lengths, the transfer of unpaired spin density, and the transition-mode frequencies (Table VIII). All TS modes show a clear movement of oxygen to nitrogen and vice versa. A geometry dependence of spin uncoupling and spin transfer has been found for O(³P) + H₂,³⁵ and this may partly account for the TS variations.

As shown in Table VIII, activation energies increase as the number of methyl groups increase from one to three. Referring to Table VII, methyl radical dissociation is more exothermic with increasing number of methyl groups, even if its lower experimental enthalpy value is used for the calculations. The different routes are compared, with equilevelling of reactants, in Figure 8. Under thermodynamic control, if possible, hydroxylamine-recombined products are slightly preferred.

Thus our results suggest that for both singlet and radical pathways, addition of the oxygen to the nitrogen in the gas phase is the determining step in hydroxyamine and methoxyamine formation. Both types of products can be formed by both pathways, but by different mechanisms and via different intermediates.

Results of gas-phase oxidations of methylamines with O(³P)^{37,38} gave the reverse order at 298 K (TMA:DMA:MMA relative rates were 39:11:1)³⁷ than that predicted from our results in Table VIII. However, intermediates and products were not identified and so the reactions measured may not have been those involving N-oxidation forming *N*-hydroxyl and *N*-methoxyl products. NH₃ required a large activation energy,³⁸ which is either for N–O bond formation or H abstraction, both ultimately probably forming hydroxylamine.

In contrast to the closed-shell pathway, oxygen addition to N via a radical mechanism is not the only pathway found. As shown in Figure 10 and in Tables IX and X, two competing reactions—H abstraction from the nitrogen and from the α -methyl carbon atom—were also characterized for methylamine.

Each TS mode shown in Figure 10 is nearly "pure" hydrogen displacement toward the oxygen, which makes each of them quite similar to hydrogen abstraction from CH₄ and from the methyl group of propene.²³ As shown in Tables IX and X, hydrogen abstraction from nitrogen (eq 16) is not thermodynamically favored with respect to abstraction from carbon (eq 15), and it is significantly slower than it and than N-oxidation (eq 12). The calculated activation free energies for C–H H-abstraction (eq 15) and N-oxidation (eq 12) are essentially the same. The enthalpy of formation for OH has an error of some 9 kcal/mol (0.2 by MNDO, 9.4 experimental value²¹) which leads to overestimates of the exothermicity of ΔG_r and underestimates of the barriers. However, for N–H abstraction, kinetic properties may make it a less favorable path than its thermodynamic properties.³⁹

In general, the results obtained suggest that α -C oxidation by H-abstraction leading to *N*-alkylol formation is slightly preferred kinetically and definitely favored thermodynamically over amine oxidation either by oxygen addition to or H-abstraction from the

nitrogen. This preference is expected to increase for dimethylamine and trimethylamine (neither calculated), since the ΔG^\ddagger for α -C H-abstraction is not expected to follow, at least quantitatively, the increase in ΔG^\ddagger calculated for N-oxidations with further substitutions. Of the two mechanisms for N-oxidation, addition of oxygen to nitrogen appears to be kinetically favored over the N–H abstraction pathway to hydroxylamine formation.

The results obtained for methylamine oxidations should be most applicable to gas-phase reactions, and a comparison with such experiments would be most instructive. Unfortunately, no experimental values are yet available for activation enthalpies and entropies for the specific reaction pathways modeled. This lack of data prohibits the calibration of MNDO results for these reactions as was possible in previous model oxidation studies.²³

The results that are available from experiments are, unfortunately, not illuminating and may be in conflict with each other. From the increasing rates with further alkyl substitution of reactions of MMA, DMA, and TMA with O(³P), Atkinson and Pitts³⁷ concluded that N–H abstraction is not a predominant pathway. They suggested, as our results do, that the results of C–H abstraction or an "addition adduct", probably the *N*-oxide, could be the initial product. As no product analysis was attempted, the observed rates cannot be connected to a defined pathway.

In an attempt to refine these results, Gutman and co-workers¹² found that, upon oxidation, (CD₃)₂NH lost hydrogen only from nitrogen. However, at least for DMA and TMA, H-abstraction appeared to follow an initial addition step. They assumed that an *N*-oxide could partly account for the observed addition adducts. These inferences from experiment are partially substantiated by our results. We also conclude that N–H abstraction would not be a predominant pathway and that C–H abstraction or addition pathways could occur and would be competitive. The observation that NH abstraction can occur only via an addition step is also consistent with the results obtained. However, we do not find an *N*-oxide intermediate in the radical pathway. Moreover, in the experimental study, no chemical analysis was performed, so that the nature of the adducts formed remains obscure. Thus whether or not *N*-oxide intermediates are formed by O(³P) oxidation of methylamines is still unresolved.

The formation of *N*-oxide intermediates requires either inter-system spin crossing (isc) to the closed-shell configuration or the existence of a meta-stable triplet adduct intermediate. As stated, in spite of our search for such intermediates, none were found on the triplet surface. Thus only the triplet \rightarrow singlet "forbidden" isc remains as a possibility. While we did not consider this process explicitly, some aspects of our results indicate it to be a reasonable alternative. In the *N*-oxide transition states on the triplet surfaces, N–O distances are shorter than on the singlet surfaces and there is substantial spin delocalization from the oxygen to the amine. About one electron spin is transferred in NH₃ decreasing to 0.6 electron spin in the trimethylamine. These factors could enhance spin-orbit coupling and hence decrease the lifetime of the excited spin states.⁴⁰ Since the rates of reaction to form the radicals are slow, adduct lifetimes may be long enough to allow the spin transitions to occur as nonradiative intersystem crossings.

In addition to direct comparisons with gas-phase oxidation, the "gas-phase" model reactions characterized may also provide some insights into enzymatic oxidations. Their relevance to such reactions is most likely greater than to reactions in polar solvents since many enzymatic active sites, including cytochrome P450s, are known to be hydrophobic and act on nonpolar substrates.⁴¹

If the "oxene" atom transferred to amine substrates has a singlet oxygen character, a number of inferences can be reached as a result of these calculations.

(1) The major role of the enzyme is to create a singlet oxygen atom. This highly excited species then allows rapid formation of *N*-oxides with very small free energies of activation.

(35) Bader, R. F. W.; Gangi, R. A. *J. Am. Chem. Soc.* **1971**, *93*, 1831.

(36) "Handbook of Chemistry and Physics", 63rd ed.; CRC Press: FL, 1982.

(37) Atkinson, R.; Pitts, J. N., Jr. *J. Chem. Phys.* **1978**, *68*, 911.

(38) Kirchner, K.; Merget, N.; Schmidt, C. *Chem. Ing. Technol.* **1974**, *46*, 661.

(39) Zabicky, J. In "The Chemistry of the Amino Group"; Patai, S., Ed.; Interscience: New York, 1968.

(40) Quina, F. H. In "Chemical and Biological Generation of Excited States"; Adam, W., Cilento, G., Eds.; Academic Press: New York, 1982.

(41) Hansch, C.; Lien, E. J.; Helmer, F. *Arch. Biochem. Biophys.* **1968**, *128*, 319.

(2) An addition–rearrangement pathway involving an *N*-oxide is the most likely one to formation of hydroxylamine products.

(3) Not only hydroxylamine but alkoxyamine products can be formed from *N*-oxides by transfer of alkyl groups from the nitrogen to the oxygen.

(4) Formation of *N*-hydroxy- or *N*-methoxyamine products from *N*-oxide intermediates while requiring large energies of activation can occur in two different ways: (a) at the hydrophobic substrate binding site from very energetic *N*-oxides formed; (b) outside the active site if the *N*-oxide loses energy to surrounding amino acid residues. In such a case, previous studies¹³ indicate solvent-assisted mechanisms of H-migration can reduce the energy barrier.

The results here yield a highly positive hydrogen in the transition state, TS2, leading to rearrangement, also indicating a solvent-assisted mechanism would be efficacious. This highly positive hydrogen in the TS will attract H₂O molecules and reduce the energy barrier. Our calculations show a decrease in oxygen and hydrogen charges in the TS-2 with increased alkylation, as the number of available hydrogens on the nitrogen is decreased. Both effects favor better assistance by water for less substituted amines, e.g., NH₃ will be the fastest to form hydroxylamine by this mechanism. Solvent-assisted migration of methyl is less important as less charge is involved, and thus the reactants are more stable with respect to such a TS. Only slight differences were found among the charges of migrating methyl groups, so selectivity is not expected, except for a statistical factor due to the number of methyl groups.

Differences in the behavior of amines in the gas phase and in solution have been noted for a simple protonation reaction. In water, TMA and NH₃ are of equal basicity, while MMA and DMA are stronger bases of similar strength. In the gas phase,⁴² basicities increase with alkyl substitutions. As gas-phase protonations are largely due to pure electrostatic attractions, the MNDO calculated charges for the parent amines show the correct order.

A radical mechanism for enzymatic oxidation of alkylamines cannot be ruled out at this stage. In this context, three competing pathways were characterized: (1) H abstraction from α -C atoms leading to *N*-alkylol and *N*-demethylation products; (2) H-abstraction from and (3) oxygen addition to nitrogen leading to *N*-hydroxyl and *N*-methoxy products.

If the oxene atom transferred to amine substrates has a radical character, our results suggest the following:

(1) α -C hydroxylation and *N*-oxidations would be competitive with *N*-oxidations occurring more in 1° > 2° > 3° amines.

(2) Of the two mechanisms leading to hydroxylamine or methoxyamine products, an *N*-addition pathway is preferred over an *N*-H abstraction pathway.

(3) The *N*-addition pathway does not lead to a stable triplet *N*-oxide intermediate. Instead, radical intermediates with a single unpaired spin are formed by loss of H or CH₃ radicals. The only way that *N*-oxide intermediates can be formed is by intersystem crossing, possibly by a spin–orbit coupling mechanism.

(4) Not only hydroxylamine but alkoxyamine products can be formed by rapid radical recombination of the doublet intermediates and H or CH₃ radicals. Such recombination could occur in the hydrophobic enzyme substrate binding site of the enzyme, would be rapid, and would not require solvent assistance.

The results obtained thus far are most consistent with a radical mechanism for oxidation of alkylamines by cytochrome P450. *N*-Demethylation of alkylamine via α -C hydroxylation is well established, consistent with the pathway favored in radical mechanisms, while evidence for *N*-oxidation of alkylamines by cytochrome P450 is more equivocal.

If a radical mechanism is favored by the enzyme, products of both *N*-dealkylation and *N*-oxidation can be formed without *N*-oxide intermediates and can occur in a hydrophobic environment. If a singlet mechanism is preferred, products of *N*-oxidation are formed with *N*-oxide intermediates and can be solvent assisted.

The need for further experiments, with complete identification of intermediates and products for the elucidation of amine oxidation mechanisms, cannot be overemphasized. Special effort should be directed to the trapping of *N*-oxide intermediates in enzymatic and in solution studies in solvents with varying polar characterization. A proper variation of solvent polarity or the addition of nonpolar species such as tetralkylammonium or large metal cations may differentially stabilize reactants, transition states, and products. Such studies should help to further distinguish between radical and nonradical mechanisms of oxidation of alkylamines.

Acknowledgment. Helpful discussions with Dr. Dale Spangler and his MNDO program modification and support for the work from NIH Grant No. GM 27943 are gratefully acknowledged.

Supplementary Material Available: A complete set of optimized geometries (and Mulliken population charges) for all reactants, transition states, intermediates, and products (Figures 1S–5S), and calculated thermochemical quantities for all reactants, intermediates, and products studied, along with comparisons with experimental values, where possible (Tables IS–VS) (18 pages). Ordering information is given on any current masthead page.

(42) Bohme, D. K. In "The Chemistry of Amino, Nitroso and Nitro Compounds and their Derivatives", Part 2; Patai, S., Ed.; J. Wiley and Sons: New York, 1982.